Expert Opinion on Drug Delivery

ISSN: 1742-5247 (Print) 1744-7593 (Online) Journal homepage: http://www.tandfonline.com/loi/iedd20

Cell-penetrating self-nanoemulsifying drug delivery systems (SNEDDS) for oral gene delivery

Arshad Mahmood, Felix Prüfert, Nuri Ari Efiana, Muhammad Imtiaz Ashraf, Martin Hermann, Shah Hussain & Andreas Bernkop-Schnürch

To cite this article: Arshad Mahmood, Felix Prüfert, Nuri Ari Efiana, Muhammad Imtiaz Ashraf, Martin Hermann, Shah Hussain & Andreas Bernkop-Schnürch (2016) Cell-penetrating self-nanoemulsifying drug delivery systems (SNEDDS) for oral gene delivery, Expert Opinion on Drug Delivery, 13:11, 1503-1512, DOI: 10.1080/17425247.2016.1213236

To link to this article: http://dx.doi.org/10.1080/17425247.2016.1213236

EXPERT OPINION ON DRUG DELIVERY, 2016
VOL. 13, NO. 11, 1503–1512
http://dx.doi.org/10.1080/17425247.2016.1213236

Taylor & Francis
Taylor & Francis Group

ORIGINAL RESEARCH

Cell-penetrating *self-nanoemulsifying drug delivery systems* (SNEDDS) for oral gene delivery

Arshad Mahmood[a], Felix Prüfert[a], Nuri Ari Efiana[a], Muhammad Imtiaz Ashraf[b,c], Martin Hermann[d], Shah Hussain[e] and Andreas Bernkop-Schnürch[a]

[a]Center for Chemistry and Biomedicine, Department of Pharmaceutical Technology, Institute of Pharmacy, University of Innsbruck, Innsbruck, Austria; [b]Daniel Swarovski Research Laboratory, Department of Visceral, Transplant and Thoracic Surgery, Medical University Innsbruck, Innsbruck, Austria; [c]Department for General, Visceral and Transplantation Surgery, Campus Virchow-Klinikum, Charité Universitätsmedizin, Berlin, Germany; [d]Department of Anesthesiology and Critical Care Medicine, Medical University Innsbruck, Innsbruck, Austria; [e]Institute of Analytical Chemistry and Radiochemistry, University of Innsbruck, Innsbruck, Austria

ABSTRACT

Objective: The aim of study was to investigate whether cell-penetrating peptides could amplify cellular uptake of plasmid DNA (pDNA) loaded self-nanoemulsifying drug delivery systems (SNEDDS) by mucosal epithelial cells, thereby enhancing transfection efficiency.

Methods: HIV-1 Tat peptide-oleoyl conjugate (TAT-OL) was synthesized through amide bond formation between HIV-1 Tat-protein 49–57 (TAT) and oleoyl-chloride (OL). SNEDDS formulation contained 29.7% each of Cremophor EL, Capmul MCM and Crodamol, 9.9% propylene glycol and 1% TAT-OL. SNEDDS with OL instead of TAT-OL served as control.

Results: Fluorescent-microscopy demonstrated 0.5% (m/v) nanoemulsions were suitable for subsequent studies. Mucus diffusion of nanoemulsion loaded with fluorescein diacetate (FDA) was 1.5-fold increased by incorporation of TAT-OL. Confocal microscopy confirmed that droplets of nanoemulsions were successfully internalized. Furthermore, quantitative analysis showed that addition of TAT-OL increases uptake of nanoemulsions by 2.3- and 2.6-folds after 2 and 4 hours of incubation, respectively. Cellular internalization pathways were found with substantial decrease in uptake in presence of indomethacin and chlorpromazine. Transfection efficiency investigated on HEK-293-cells was found to be 1.7- and 1.8-fold higher for SNEDDS loaded with TAT-OL compared to Lipofectin and control, respectively.

Conclusion: In comparison to prevailing lipid and polymer-based delivery systems, these novel cell-penetrating SNEDDS likely represent most effective, simplistic and expedite dosage form for mucosal gene delivery.

ARTICLE HISTORY
Received 6 April 2016
Accepted 16 June 2016
Published online
3 August 2016

KEYWORDS
Cell-penetrating peptide; HIV-1 Tat protein; SNEDDS; cellular internalization; transfection efficiency

1. Introduction

Gene therapy involves introduction of genetic material at target sites to regulate the manifestation of specific proteins. Effective gene therapy requires potential vectors to deliver the genetic material [1,2]. High transfection rates could be accomplished with viral gene delivery systems; however, safety concerns particularly oncogenicity and immunogenic effects limit their use [3]. Nonviral gene delivery is achieved by numerous nanocarriers including liposomes, microcapsules, polymer-based nanoparticles, polycation complexes, and self-nanoemulsifying drug delivery systems (SNEDDS) [4,5].

The fundamental challenges with nonviral gene delivery systems are poor cellular uptake and enzymatic degradation of DNA-based drugs, particularly through oral route [6,7]. SNEDDS have principally been explored for oral delivery of lipophilic drugs [8]. Recently, however, they have been investigated for delivery of genetic material as well. Hydrophobic ion-paired pDNA being incorporated in SNEDDS was protected toward enzymatic degradation compared to naked pDNA and pDNA–lipid complexes. Moreover, the transfection efficiency of SNEDDS was as effective as Lipofectin®, used as gold standard transfection reagent [5]. A promising approach to further boost the transfection efficacy is the use of cell-penetrating peptides (CPPs) derived from proteins that are able to cross cell membranes. CPPs have been used for transportation of various drug carriers including nanoparticles and liposomes into cells [9]. So far, however, the potential of the combined use of SNEDDS and CPPs has not been evaluated.

It was therefore the aim of this study to combine these two promising strategies in one formulation and to investigate its impact on cellular internalization and transfection efficiency. Among CPPs, TAT was chosen as it has already been effectively used by our research group to enhance the cellular internalization of nanoparticles [10]. TAT is a nine amino acid motif (H-Arg-Lys-Lys-Arg-Arg-Gln-Arg-Arg-Arg-OH) and serves

CONTACT Andreas Bernkop-Schnürch andreas.bernkop@uibk.ac.at Center for Chemistry and Biomedicine, Department of Pharmaceutical Technology, Institute of Pharmacy, University of Innsbruck, Innrain 80/82, Innsbruck 6020, Austria

Supplemental data for this article can be accessed here.

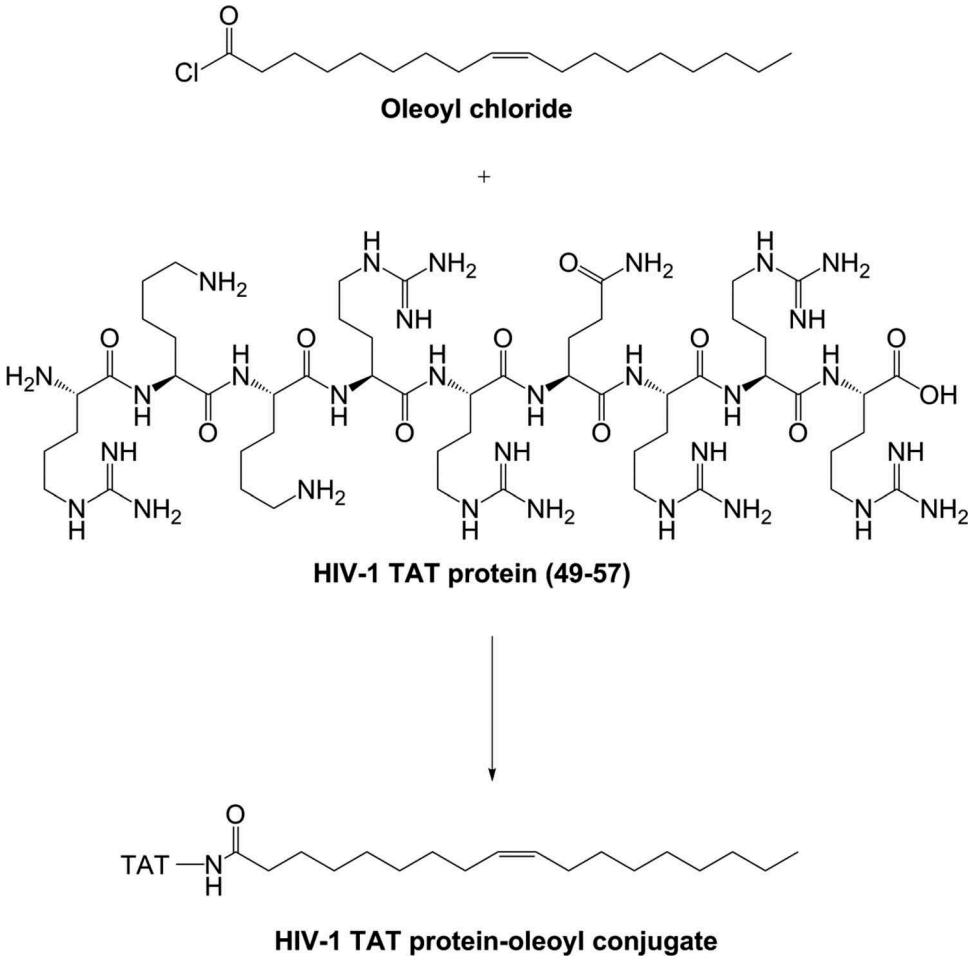

Figure 1. Synthetic pathway and presumptive chemical substructure of HIV-1 Tat protein- oleoyl conjugate (TAT-OL).

the purpose of transducing gene/DNA through the cell membrane [11,12]. It is cationic in nature and translocates genetic material across cell membranes in an energy-independent mode. TAT was made lipophilic through conjugation with OL as illustrated in Figure 1. Afterwards, nanoemulsions prepared from SNEDDS containing TAT-OL were explored regarding their physicochemical properties, cytotoxic potential, mucus diffusion behavior, qualitative and quantitative cellular uptake, internalization pathways, and transfection efficiency.

2. Material and method

2.1. Materials

HIV-1 Tat protein (49–57) was obtained from GL Biochem Ltd. Shanghai, China, Capmul MCM from Abitec Corporation, Janesville, USA, tetrahydrofuran from AppliChem GmbH., Ottoweg, Germany, Crodamol from Croda GmbH. Nettetal, Germany and propylene glycol from Gatt-Koller, Absam, Austria. Nile red, Cremophor EL, cetrimide and oleoyl chloride were purchased from Sigma–Aldrich, Vienna, Austria. Hoechst 33342 and propidium iodide were acquired from Molecular Probes, Eugene, USA. The green fluorescent plasmid was amplified in *Escherichia coli* supplied by Addgene (pcDNA3-EGFP, Addgene plasmid 13031). Agarose, Agar-Agar, and LB-Medium were ordered from Carl Roth, Karlsruhe Germany, the plasmid-extraction kit by Qiagen, Hilden, Germany and Lipofectin by Life Technologies, Carlsbad, CA, USA. All other reagents were of analytical grade.

2.2. Synthesis of the HIV-1 TAT protein-oleoyl conjugate

TAT-OL was synthesized through amide bond formation between a highly reactive acid halide and an amine by condensation [13]. With slight modification in method, OL was reacted in an equimolar ratio with TAT. Briefly, 22.27 mg of OL (dark brown opaque liquid) dissolved in 800 µL of tetrahydrofuran was mixed with 5 mg of TAT (white colored lyophilized powder) dissolved in 200 µL of distilled water. The blend was mixed on a vortex for 2 min and afterwards placed in thermomixer at 30°C for 1 h. The newly formed TAT-OL conjugate was separated from mixture by addition of 1 mL of distilled water. The unreacted TAT being hydrophilic in nature remains in the aqueous phase. TAT-OL (yellowish brown liquid) comprising the upper layer was decanted off and allowed to stand overnight to evaporate any entrapped organic solvent. Subsequently, the conjugate was stored at 4°C until used.

2.3. Fourier transform infrared spectroscopy

Spectra of OL and TAT-OL were obtained using a set up comprising of Perkin Elmer Spectrum 100 ATR-IR spectrometer (Perkin Elmer, Waltham, USA) in association with Spectrum software version 6.3.1.0134 (Perkin Elmer, Waltham, USA). A drop each of OL and TAT-OL was placed on the lens of the instrument, covering probe was screwed, and measurements were recorded. Both spectra were recorded with specification of 10 scans, wave number ranging from 4000 to 650 cm^{-1}, a resolution of 1 cm^{-1}, and the measurements were executed at 22°C [14].

2.4. Thin-layer chromatography

Analytical thin-layer chromatography (TLC) was performed to further confirm the conjugate formation, using precoated silica gel aluminum sheet (0.5 mm thick) acting as stationary phase. TLC plate (8 × 5 cm) was developed by applying 10 µL samples from each of OL, TAT (1% w/v in water), and TAT-OL conjugate equally separated 2 cm from the bottom and allowed them to dry. Afterwards, the plate was placed in TLC chamber and immersed in the mobile phase comprising hexane/ethyl acetate/acetic acid (80/20/1, v/v/v) in a way that sample spots remained well above the level of mobile phase. The lid was closed and mobile phase was allowed to run through the length of stationary phase for 30 min. The eluent was evaporated from the chromatogram under laminar airflow. Afterwards, the chromatogram was observed under shortwave ultraviolet light, and the illuminated spots were marked with graphite pencil. In order to visualize TAT, TLC plates were sprayed with ninhydrin reagent [0.3% ninhydrin (m/v) in ethanol].

2.5. Preparation and loading of SNEDDS

The SNEDDS formulation consisted of Cremophor EL, Crodamol, Capmul MCM, propylene glycol, and TAT-OL mixed in a mass ratio (m/m) of 3 : 3 : 3 : 1 : 0.1 [15]. The control SNEDDS were prepared in the same way but replacing TAT-OL with OL. For the *in vitro* experiments with Caco-2 cells, SNEDDS formulations were loaded either with 0.1% FDA or with 0.01% nile red. Transfection studies were performed after loading the precipitated pDNA–lipid complexes in a concentration of 0.5% (v/v) into SNEDDS.

2.6. Characterization of nanoemulsion

Nanoemulsions were prepared by diluting SNEDDS formulations with and without TAT-OL in 100 mM phosphate buffer pH 6.8 or culture medium in a final concentration of 0.5% (m/v) at room temperature. Droplet size and zeta potential of both emulsions were determined by dynamic light scattering utilizing a PSS NicomPTM 380 DLS (Santa Barbara, CA, USA) directly after preparation.

2.7. Fluorescent microscopy

Fluorescent microscopy was used to identify the optimum concentration of SNEDDS formulation for cellular uptake and transfection studies [16]. Caco-2 cells were cultured in eight-well chambered coverglass (Nalge Nunc International) at a density of 1 × 10^5 cells/mL in 300 µL of minimum essential medium (MEM) containing 20% fetal calf serum (FCS) at 37°C and 5% CO_2. MEM was replaced every 48 h until approximately 100% confluence was reached. Thereafter, cells were incubated with an increasing concentration of SNEDDS 0.1%, 0.5%, and 1.0% (m/v) diluted in the culture medium without FCS. SNEDDS contained 0.01% nile red, and pH of all nanoemulsions was adjusted to 7.4. Cells treated with culture medium only served the purpose of control. After an incubation of 4 h at 37°C, 5% CO_2, a solution of Hoechst 33342 (HO), and propidium iodide (PI) in culture medium were added separately to the contents of each well to provide final concentrations of 10 µM HO, 10 µM PI. Following an incubation of cells for 10 min with the live stains, digital images were taken using an Olympus IX-70 inverted microscope using Olympus 40× water (numerical aperture 0.8) and an Olympus U-RFL-T mercury-vapor lamp. Images were acquire and analyzed using a Kappa ACC1 camera and Kappa ImageBase software, respectively.

2.8. Mucus diffusion test

The penetrating ability of SNEDDS formulations through the intestinal mucus was analyzed by silicon tube method. Silicone tubing (Carl Roth GmbH, Karlsruhe, Germany) with an internal diameter of 3 mm in a horizontal rotating arrangement was used for this purpose. The silicon tubes were filled with 300 µL of intestinal mucus, and one end of tube was closed with small silicon cap. Thereafter, 50 µL of FDA-loaded SNEDDS dispersions in 100 mM phosphate buffer pH 6.8 were added to the open end, and the tube was sealed with another silicon cap. All tubes were placed in an incubator at 37°C in a horizontally rotation arrangement for 4 h. At the end of incubation time, the tubes were frozen by placing overnight in a freezer (−20°C). Afterwards, all silicon tubes were cut into 10 slices of 2 mm length. Each slice was suspended in 300 µL of 5 M NaOH, and after vortexing for 30 s, all samples were incubated in dark place for 30 min in order to hydrolyze FDA to sodium fluorescein (Na-flu). The resultant Na-flu was then analyzed fluorimetrically using a microplate reader (Tecan Austria GmbH, Austria. Ex 485 nm and Em 535 nm), and calculations were performed using 100% value of each SNEDDS dispersion. Silicone tubes containing fresh mucus functioned as blank, and its absorbance values were subtracted from all samples to obtain absorbance of Na-flu only.

2.9. Real-time live confocal microscopy

Caco-2 cells (1 × 10^5 cells/mL) were seeded in an eight-well chambered coverglass in 300 µL MEM. The coverglass was incubated at 37°C, and 5% CO_2 and MEM (supplemented with 20% FCS) was replaced at alternate day till confluence

was achieved. The cells were equilibrated with MEM (without FCS) pH 7.4 at 37°C for 30 min. Afterwards, medium was replaced with 0.5% (m/v) nanoemulsions of SNEDDS (loaded with 0.01% nile red) in MEM (without FCS) and incubated for 2 and 4 h. At the end of experiments, Caco-2 cells were stained for 10 min at 37°C with HO and PI in a final concentration of 10 µM of each. After incubation with the stains, cells were analyzed with a confocal microscope (510 Meta, Carl Zeiss, Jena, Germany) equipped with a diode at 405 nm of excitation, an argon laser (providing the excitation at 488 nm), and a helium/neon laser (providing the excitation at 543 nm). An oil immersion objective (40×) was used to investigate the uptake of formulation by Caco-2 cells.

Confocal images were acquired with a microlens-enhanced Nipkow disk-based UltraVIEW RS confocal scanner (Perkin Elmer, Wellesley, MA, USA) mounted on an Olympus IX-70 inverse microscope (Olympus, Nagano, Japan). Images were collected using the ULTRAVIEW LCI software version 5.4 (Perkin Elmer) [17].

2.10. In vitro *cellular uptake studies*

Cellular uptake study was executed with Caco-2 cells monolayer. For this purpose, Caco-2 cells in a concentration of 1×10^5 cells/well were seeded on 24-well plates in 500 µL culture medium (MEM supplemented with 20% FCS). The cells were incubated in an environment of 5% CO_2 at 37°C, and medium was replaced every 48 h.

After accomplishing of 100% confluence, Caco-2 cells were incubated with MEM deprived of FCS (pH 7.4) for 30 min. Upon reaching equilibrium, culture medium was exchanged with prewarmed 500 µL of FDA-loaded SNEDDS dispersions (0.5%, m/v, in MEM without FCS, pH 7.4). The exposure of Caco-2 cells with nanoemulsions continued for 2 and 4 h. At the end of the incubation time, nanoemulsions were removed, and cell monolayer was gently washed twice with prewarmed phosphate buffered saline (PBS). Cells were lysed by addition of 300 µL of 2% Triton X-100 in 5 M NaOH. The lysis treatment without the removal of the nanoemulsions was used as the corresponding 100% and cells incubated with MEM only as analogous 0%. After 30 min of incubation, the fluorescence intensity (FI) of lysate was analyzed using a microplate reader at λex = 485 and λem = 555 nm. Results of cellular uptake efficiency were expressed through equation (Equation (1)),

$$\text{Uptake efficiency}(\%) = \frac{\text{FIa} - \text{FIx}}{\text{FIc} - \text{FIx}} \times 100$$

where FIa and FIc represent FI of the lysate with and without removing nanoemulsions, respectively. FIx is FI of corresponding 0%.

2.11. Endocytosis inhibition

The potential uptake pathways of SNEDDS formulation were investigated by endocytosis inhibition block method [16]. The cellular uptake study was performed upon cells having priory been treated with endocytosis inhibitors including chlorpromazine (10 µg/mL) and indomethacin (100 µg/mL) for 30 min and later incubation with nanoemulsions for 4 h. Chlorpromazine (CPZ) and indomethacin (INM) are considered to inhibit the clathrin-mediated and caveolae-mediated endocytosis pathways, respectively. Afterwards, cells were treated in the same way as describe in Section 2.10, and cellular uptake efficiency (%) was calculated as per Equation (1).

2.12. Preparation of the plasmid

The ultimate investigation whether TAT-OL has an impact on transfection efficiency of SNEDDS was carried out with green fluorescence protein plasmid pcDNA3-EGFP (6.1 kb). The plasmid was obtained as described by Bonengel et al. [18]. Briefly, plasmid was first replicated in *E. coli* and then extracted using Midi Prep kit from Qiagen. Afterwards, the isolated pDNA was suspended in TE-buffer and concentration of the purified plasmid DNA was determined with Thermo Scientific NanoDrop 2000 spectrophotometer (Fisher Scientific, Vienna, Austria). Later, pDNA suspension was diluted with endotoxin-free demineralized water to required concentration and stored at −20°C until use.

2.13. Hydrophobic ion pairing

Prior to loading of plasmid to SNEDDS, lipophilicity of the plasmid needed to be increased by hydrophobic ion paring [5]. For this purpose, cetrimide was mixed with pDNA in a molar ratio of 2:1. The complex formation should occur due to the cationic amino group of the lipid and the negatively charged backbone of the pDNA. The mixture was vortexed, allowed to stand at room temperature for 5 min, and then centrifuged at 13,400 rpm for 10 min. The supernatant was removed, and isolated hydrophobic pDNA–cetrimide complex was loaded into SNEDDS for transfection studies.

2.14. In vitro *transfection assay*

Transfection studies were performed on HEK-293 cells to provide a better comparison in efficiency with already existing data. HEK-293 cells (4×10^5 cells/mL) were seeded in a 24-well plate in 500 µL of D-MEM and incubated in an environment of 37°C and 5% CO_2. After 24 h of incubation, SNEDDS (with OL and TAT-OL) loaded with pDNA–lipid complex were dispersed in D-MEM making 0.5% (m/v) dilution. Subsequently, 500 µL of the nanoemulsion was transferred to each well resulting in a final concentration of 0.5 µg of pDNA per milliliter. For the purpose of control, HEK-293 cells were exposed to naked pDNA and the pDNA–Lipofectin complex prepared as per specifications provided by Lipofectin supplier. After an incubation of 4 h, the supernatant was removed, and MEM containing FCS and antibiotics was used instead and incubated for 48 h. Thereafter, the cells were harvested for Green fluorescent protein (GFP) assay [5,18].

2.15. Green fluorescence protein assay

GFP assay was performed to quantify transfection efficiency as described previously by Hauptstein et al. [5]. Briefly, removal of MEM was followed by washing of cells two times with

prewarmed PBS. Thereafter, cells were treated with 100 µL of phosphate buffer 100 mM (pH 7.5) containing 0.2% Triton X-100 and 1 mM dithiothreitol and a freeze-thawing cycle leading to lysis of the cells. Then, 50 µL of lysate from each sample was shifted to a 96-well plate, and the amount of GFP was determined fluorimetrically by measuring fluorescence using a microplate reader (Tecan Austria GmbH, Austria. Ex 488 nm and Em 510 nm).

2.16. Statistical data analysis

All experiments were performed in triplicates, and outcomes are reported as the means ± SD. Statistical analysis of data was performed using Student's t-test assuming equal variance with $p < 0.01$ and $p < 0.001$ level of significance. Moreover, GraphPad Prism 5 software was used for graphical presentation.

3. Results

3.1. Synthesis and characterization of TAT-OL

The covalent attachment of TAT to OL was achieved by the formation of amide bonds between the primary amino group of TAT and acyl halide as depicted in Figure 1 (detailed chemistry is described in supplementary Figure 1). The TAT-OL conjugate appeared as light brown opaque liquid with weak irritating odor. The newly synthesized conjugate was characterized by FTIR and TLC. The FTIR spectrum of OL and TAT-OL is described in Figure 2. The unmodified OL is reflected by the distinctive bands at 2800–2950 cm^{-1} (C–H stretching), 1800 cm^{-1} (C=O, acyl chloride), and TAT-OL is characterized by additional bands including 2500–3500 cm^{-1} (O–H stretching), 3000–3300 cm^{-1} (N–H stretch), 1710 cm^{-1} (C=O stretching, amide), and 1180–1350 cm^{-1} (C–N stretching). Bands were designated to be in accordance with those reported by Maquelin et al. [19] and Chaffanjon et al. [20] having obtained very similar bands for the same substructure. Furthermore, the conjugate formation was qualitatively confirmed by TLC analysis of OL, TAT, and TAT-OL as shown in Figure 3. The chromatogram was observed under shortwave ultraviolet light where OL and TAT-OL displayed their movement as illuminating bright spot extending along the length of the plate. Later, with the application of ninhydrin reagent, TAT appeared as a big dark purple spot at its area of application, i.e. it did not move along the mobile phase. TAT-OL displayed small scattered purple spots distancing 1–4 cm from its area of application and in the same illuminating region marked under ultraviolet light.

3.2. Preparation of SNEDDS and characterization of the nanoemulsion

Control and TAT-OL containing SNEDDS formulation were loaded with different fluorescent markers and pDNA independently. All the loaded and empty SNEDDS formulations were diluted in 100 mM phosphate buffer pH 6.8 resulting in a slightly bluish nanoemulsion. The mean diameter (intensity weight) of droplets in the nanoemulsion was not affected by TAT-OL and remained around 35 nm; however, it increased to around 50 nm after loading with pDNA. Zeta potential values for all nanoemulsions remained neutral to slightly negative. Details of mean droplet size and zeta potential are described in Table 1. There was only a slight change in size distribution after loading with fluorescent markers. The nanoemulsion remained stable over an observation period of 24 h and no significant change in size distribution and zeta potential could be observed. Furthermore, the droplet size and zeta potential values of nanoemulsions diluted in MEM for various cellular studies also showed an insignificant difference as compared to observation in buffer.

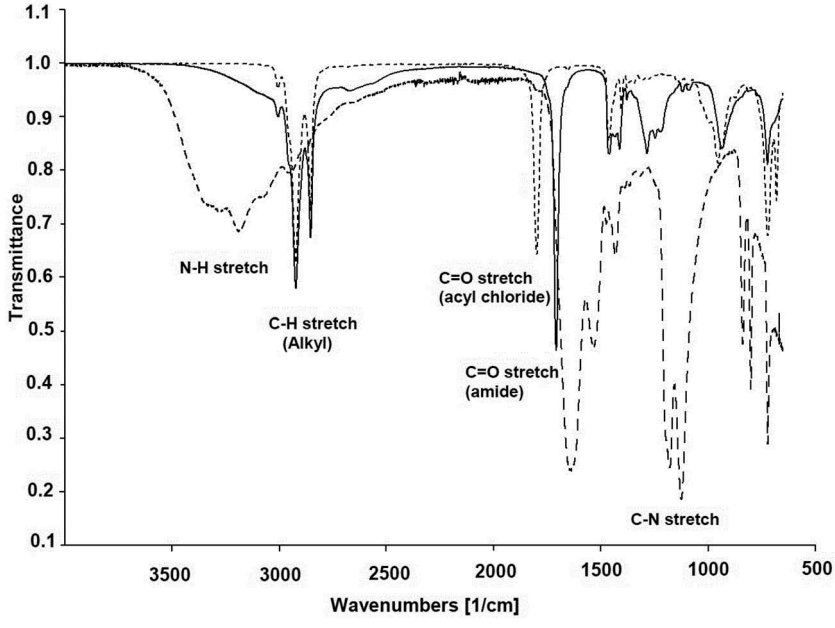

Figure 2. FTIR spectra of HIV-1 Tat protein- oleoyl conjugate [solid line], HIV-1 Tat protein [dashed line] and oleoyl chloride [dotted line].

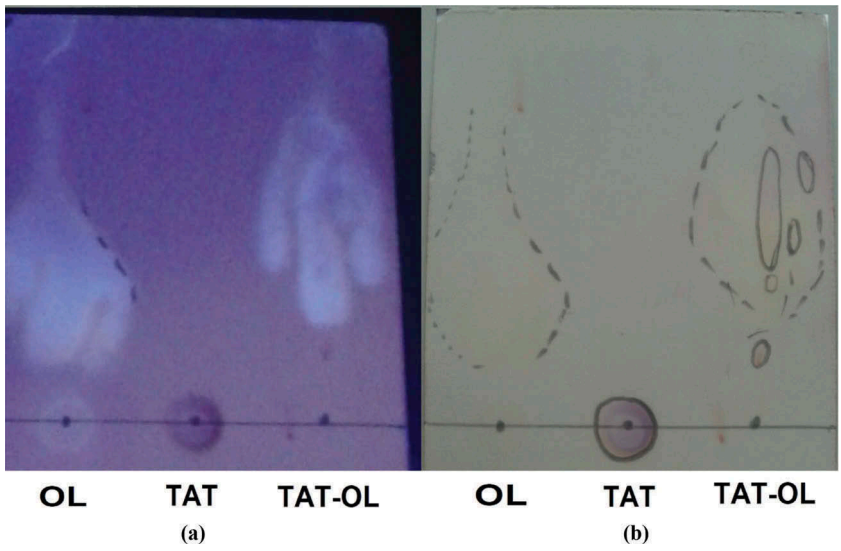

Figure 3. Thin layer chromatography of oleoyl chloride (OL), HIV-1 Tat protein (49–57) (TAT) and HIV-1 Tat protein-oleoyl conjugate (TAT-OL) (**a**) view under ultra violet light (**b**) view to naked eye.

Table 1. Amount of indicated components used for SNEDDS formulations and their characterization in terms of droplet size and zeta potential when being diluted 1:200 in 100 mM phosphate buffer pH 6.8.

	Kolliphor (mg)	Capmul MCM (mg)	Crodamol (mg)	Propylene glycole (mg)	OL (mg)	TAT-OL (mg)	pDNA (µg)	Droplet size (nm)	Zeta potential (mV)
F-1	300	300	300	100	10	-	-	35.5 ± 8.37	−0.52
F-2	300	300	300	100	-	10	-	37.7 ± 9.07	−0.01
F-1$_{pDNA}$	300	300	300	100	10	-	250	51.5 ± 23.39	−2.23
F-2$_{pDNA}$	300	300	300	100	-	10	250	53.8 ± 21.93	−1.29

3.3. Cytotoxicity analysis

Fluorescent microscopic live–dead cell analysis involving combination of HO and PI was used to determine optimum concentration of SNEDDS on Caco-2 cells. The visuals obtained from the microscope are presented in Figure 4. DNA/nucleus was stained by Hoechst nuclear dye and appeared as blue under the microscope. PI was able to penetrate the compromised cell membrane when nanoemulsion was used in 1% (m/v) concentration, not at 0.1% or 0.5% (m/v). The characteristic red spots visible at 0.1% (m/v) and 0.5% (m/v) concentration owe to be nanoemulsion droplets, further confirmed by merger with HO showing them to be in cytoplasm. The association of nile red itself with cells was also investigated through fluorescent microscopy serving as control. No red signal was detected indicating that this probe alone was not internalized into Caco-2 cells within 4 h.

3.4. Mucus diffusion studies

The influence of TAT-OL on the transport capacity of SNEDDS was explored using silicon tubes. In this technique, nanoemulsions stay in direct contact with the mucus, and the results obtained are shown in Figure 5. Inclusion of TAT-OL increased the diffusion ability of the SNEDDS in quantitative terms. The difference in penetration capacity is predominantly visible in segments 1–4, where approximately 30% of F-2 penetrated in the mucus layer as compared to just 20% of F-1.

3.5. Cellular uptake profile

The uptake efficiency of nanoemulsion was qualitatively observed by confocal microscopy. The stain HO added prior to confocal microscopic observation gave strong green signal demonstrating the location of nuclei. Red signal was observed at the periphery of cell nuclei in an increasing strength as the incubation time with nanoemulsion increased. Thereafter, a three-dimensional analysis of the optical sections (z-axis) of the cell monolayer was performed to determine the intracellular distribution of nanoemulsion. Figure 6 demonstrates that a strong red signal can be detected in the cytoplasm rather than around the cell membrane, showing that the majority of nanoemulsion droplets are accumulated in the cytoplasm. No nanoemulsion droplets were detected inside the cell nuclei, and this may have contributed to low toxicity. Furthermore, evaluation of cellular uptake of nile red by Caco-2 cells demonstrated that this probe alone is not internalized as no red fluorescent signal could be observed.

Cellular uptake of nanoemulsions F-1 and F-2 loaded with FDA is depicted in Figure 7. The internalization of nanoemulsions into Caco-2 cells was assessed by means of fluorescence intensity of Na-flu formed by activation of FDA with NaOH. An enhancement of 2.3-fold and 2.6-fold was observed with TAT-

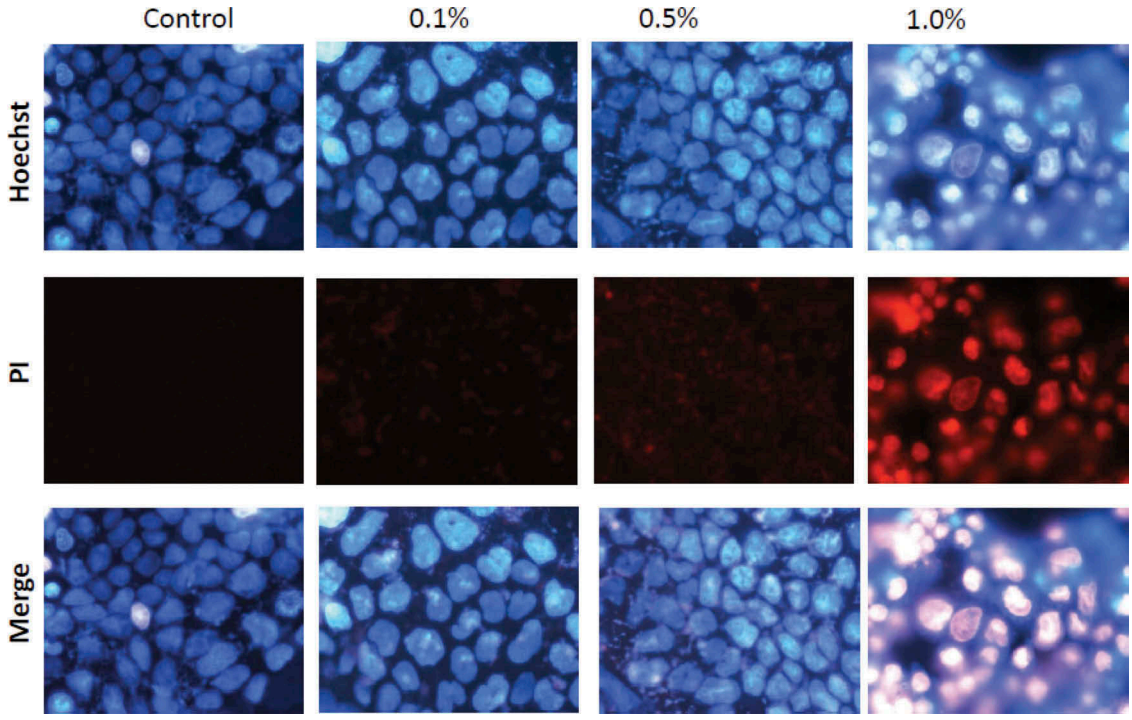

Figure 4. Fluorescent microscopic images of different concentration (0.1%, 0.5%, 1.0%) of SNEDDS loaded with nile red and control. Hoechst and propidium iodide (PI) were added just before analysis.

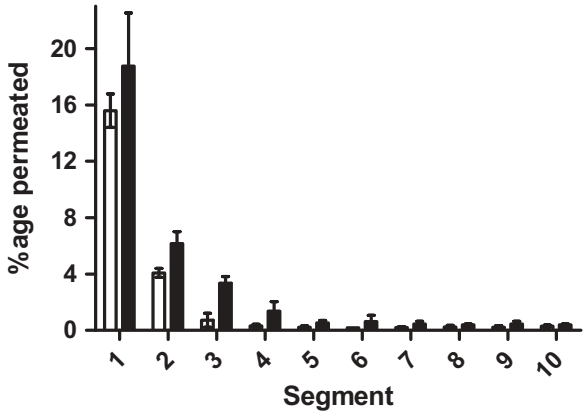

Figure 5. Diffusion studies of FDA labeled SNEDDS formulations F-1 (white bars) and F-2 (black bars) with rotating silicon tube method at 37°C over 4 h. Indicated values are means ± SD (n = 3).

OL in uptake efficiency of nanoemulsion after 2 and 4 h of incubation, respectively. Furthermore, the pathway by which these nanoemulsions are internalized was studied by using endocytosis inhibitor block model, and results are illustrated in Figure 8. With their individual treatment, CPZ led to a 50.5% decrease in uptake efficiency of control nanoemulsions and INM decreased by 29.8%. Uptake efficiency of the nanoemulsion containing TAT-OL under same conditions was decreased by 61.5% and 39.9% for CPZ and INM, respectively.

3.6. Transfection studies

GFP assay was performed 48 h after the incubation with nanoemulsions F-1_{pDNA}, F-2_{pDNA}, and various controls. The outcome of GFP assay is shown in Figure 9. Both nanoemulsions exhibited considerably enhanced transfection compared to naked pDNA. Amount of GFP expressed after transfection with F-1_{pDNA} was analogous to that of Lipofectin. However, after an incubation period of 4 h, transfection efficiency of F-2_{pDNA} was enhanced by 1.76-fold and 1.67-fold in comparison to F-1_{pDNA} and Lipofectin, respectively. Statistically, this escalation is significantly different ($p < 0.01$).

4. Discussion

A predominant component in cell-penetrating SNEDDS is TAT that has been conjugated with OL (halide derivative of oleic acid) through amide bond formation to make it lipophilic. Coupling of acyl chlorides to amines is in most cases sufficiently vigorous under aqueous conditions, although the reaction may be hastened using a catalyst [21]. FTIR spectra confirmed the conjugate formation with characteristic changes like N–H stretch, C–N stretch, and shift in C=O stretch because of secondary amide formation. Furthermore, TLC was explored as a different method to confirm the conjugation. A nonpolar solvent system was chosen in such a way that OL moved freely along with solvent and free TAT exhibited strong affinity toward stationary phase and did not move. However, violet traces with ninhydrin 1–4 cm from the area of application and in the same zone as OL endorse TAT-OL conjugate formation.

To study the impact of CPP on uptake/transfection efficiency of SNEDDS, an already developed stable SNEDDS formulation [7] was used with little modification to incorporate TAT-OL. Particle size and zeta potential remained almost unaffected with loading of TAT-OL. The slight negative zeta potential may be attributed to oleic acid like co-emulsifier properties

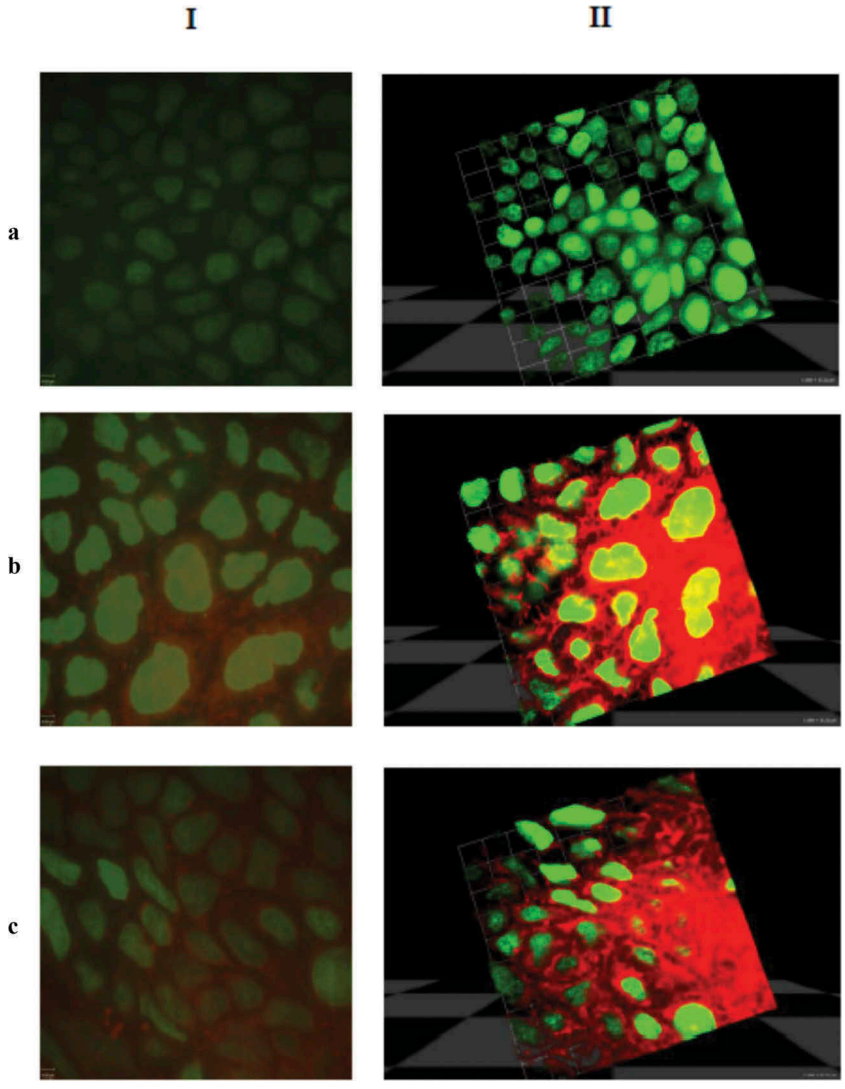

Figure 6. Confocal images (I) live imaging and (II) three dimensional view of Caco-2 cells monolayer incubated with nile red loaded SNEDDS formulation (a) control, (b) 2 h (c) 4 h incubation at 37°C and 5% CO_2. Hoechst was added and incubated for 10 min before analysis to mark the nucleus.

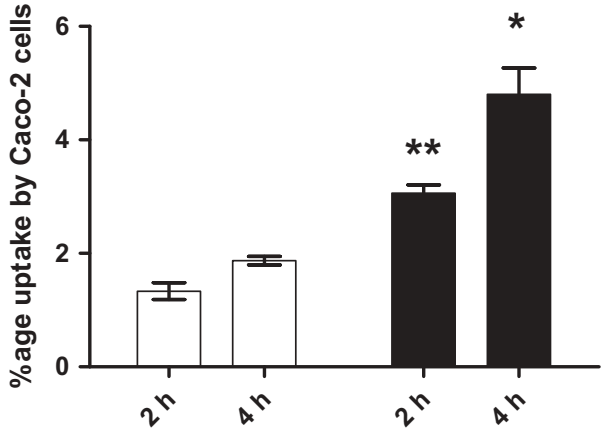

Figure 7. A comparison of uptake efficiency of SNEDDS formulations F-1 (white bars) and F-2 (black bars) after an incubation of 2 and 4 h upon Caco-2 cell monolayers in an atmosphere of 5% CO_2 at 37°C. Data represented mean ± SD, n = 3. (* $p < 0.01$, ** $p < 0.001$).

of OL that could accumulate at the interface and possess few negatively charged ionized carboxyl groups [22]. It becomes more negative after loading of cationic pDNA–cetrimide complex.

The cell viability assay accomplished in this study comprised concentration gradient of SNEDDS and simultaneous use of three fluorescent dyes nile red, HO, and PI. Nile red was incorporated in SNEDDS, whereas HO and PI dissolved in culture medium were added directly to Caco-2 cells at the end of incubation period. HO is a fluorescent marker that illustrates the position of nuclei of all cells. PI is impermeable to cell membrane and therefore does not enter viable cells with intact membranes. However, once PI advances to the nucleic acids of cells with compromised cell membrane, its fluorescence escalates vividly [23]. Consequently, this approach was used to establish optimum concentration of SNEDDS for upcoming cellular studies at which Caco-2 cells remain viable.

It is believed that positively charged particles are stuck in the mucus, while negatively charged particles can permeate through the mucus layer, and furthermore, it is established that neutral particles show even higher permeation than negative particles [24,25]. Both the nanoemulsions F-1 and

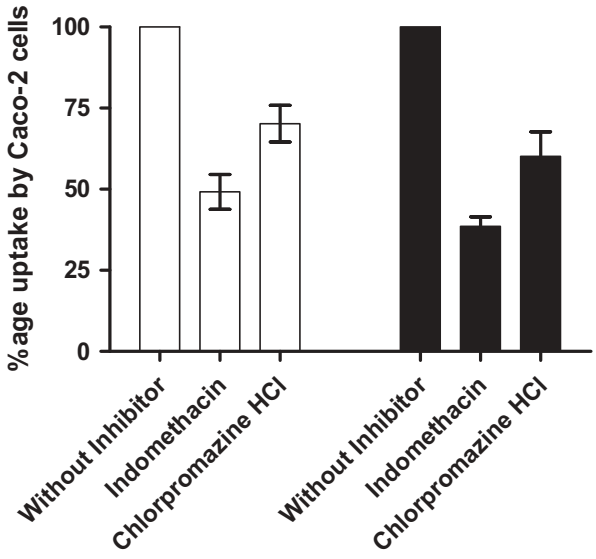

Figure 8. Impact of inhibitors on cell uptake of SNEDDS formulations F-1 (white bars) and F-2 (black bars) after an incubation of 4 h upon Caco-2 cell monolayers in an atmosphere of 5% CO_2 at 37°C. Data represent mean ± SD, n = 3.

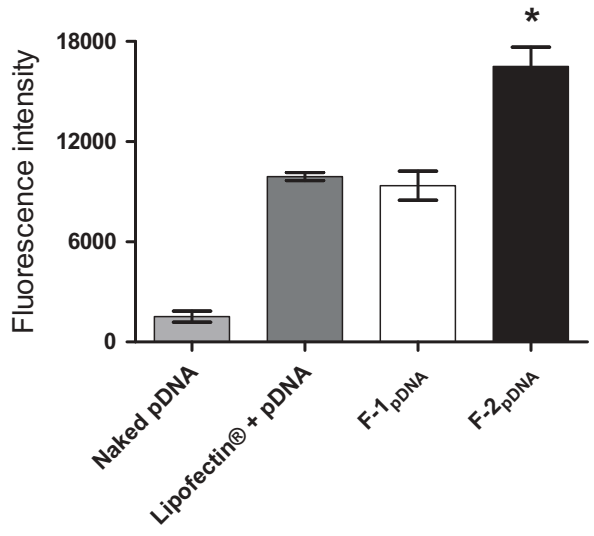

Figure 9. Transfection studies on HEK-293 cells over a period of 4 h. Cells were harvested for green fluorescence protein 48 h after transfection and fluorescence intensity was measured after cell lysis using a microplate reader (488 excitation/510 emission wavelength). Indicated values are means of three replicates ± SD. (* $p < 0.01$).

F-2 exhibited a slightly negative zeta potential, with latter closer to neutral values. Therefore, the mucus permeation capability was slightly improved after incorporation of TAT-OL.

The internalization of nanoemulsion labeled with nile red into the Caco-2 cells was confirmed under real-time live confocal microscopy. Moreover, quantitative analysis demonstrated significant improvement in the amount of internalized FDA loaded into nanoemulsions. Most nonviral drug delivery systems cannot pass freely through the cell membrane [26]. Furthermore, cellular interactions of these delivery systems are highly dependent on their structure. Liposomes, for instance, have been shown to interact through liposome–cell fusion and/or endocytosis [27]. Similarly, nanoparticles are suggested to be internalized by the cell through one or several distinct endocytosis pathways [28]. Answering the question how nanoemulsions gain entry into cells can have a high impact for a rational design of such nonviral drug delivery systems. Endocytosis has been a well-known mechanism for internalization of extracellular material into the cells. Endocytosis is generally classified into clathrin-dependent, caveolae-mediated, micropinocytosis and clathrin-independent, and caveolae-independent endocytosis [26,29,30]. The pathways for internalization of nanoemulsions found by using pharmacological inhibitor block method suggested that nanoemulsions are reaching the cytoplasm after being transported by multiple endocytosis pathways. In this study, we employed CPZ and IND as inhibitors of clathrin-mediated and caveolae-mediated pathways, respectively. CPZ redistributes clathrin from the cell membrane making it unavailable for assembly at the cell surface [31], and IND inhibits the internalization of caveolae and the return of membrane vesicles to the cell surface [29]. A total of approximately four-fifth of uptake of F-1 was inhibited with independent use of IND and CPZ. However, this inhibition reaches nearly 100% in case of F-2, demonstrating that TAT-OL largely increases caveolae-mediated and clathrin-mediated transport to a level that all other pathways become negligible. The mechanism involved in this enhancement is not completely understood; however, the possible means could be strong binding affinity of TAT toward heparin sulfates on the cell surface. It has generally been established that cells relying on uptake of exogenous polyamines exhibit heparin sulfate proteoglycans on cell surface with increased polyamine affinity [32]. Like viral particles, it may specifically bind to glycosaminoglycan-specific structures of heparin sulfate, an initial development in the direction of protein translocation [33,34]. Heparin sulfate-dependent endocytosis is not limited to any single pathway, and it varies with cellular context and extracellular molecules [32]. In a similar way, TAT-OL might enhance cellular uptake of nanoemulsions into Caco-2 and HEK-293 cells.

5. Conclusion

Numerous delivery systems differing in terms of structure, size, and chemistry have been developed to elucidate the delivery problems of DNA-based drugs. In parallel to existing lipid-based complex vectors or polymer-mediated delivery systems, we present cell-penetrating SNEDDS for mucosal epithelial delivery of DNA based drugs. The combination of two strategies, i.e. SNEDDS and CPP has not been reported before. In principle, these novel SNEDDS are cost-effective, easy to produce, provide stability against enzymatic degradation, and their transfection efficiency is superior to existing drug delivery systems and standard transfection agents. With these remarkable properties, cell-penetrating SNEDDS are in a strong position to be considered as potent and noncytotoxic carrier for DNA-based drugs.

Funding

The authors are thankful and would like to extend acknowledgement to the Higher Education Commission of Pakistan (HEC) and the Austrian Agency for International Cooperation in Education and Research (ÖAD) for their support and funding (ICM-2014-09718).

Declaration of interest

The authors have no other relevant affiliations or financial involvement with any organization or entity with a financial interest in or financial conflict with the subject matter or materials discussed in the manuscript apart from those disclosed.

References

Papers of special note have been highlighted as either of interest (•) or of considerable interest (••) to readers.

1. Ozbas-Turan S, Aral C, Kabasakal L, et al. Co-encapsulation of two plasmids in chitosan microspheres as a non-viral gene delivery vehicle. J Pharm Pharm Sci. 2003;6:27–32.
2. Crystal RG. Transfer of genes to humans: early lessons and obstacles to success. Science. 1995;270:404–410.
3. Mansouri S, Lavigne P, Corsi K, et al. Chitosan-DNA nanoparticles as non-viral vectors in gene therapy: strategies to improve transfection efficacy. Eu J Pharm Biopharm. 2004;57:1–8.
4. Fahr A, Liu X. Drug delivery strategies for poorly water-soluble drugs. Expert Opin Drug Del. 2007;4:403–416.
5. Hauptstein S, Prüfert F, Bernkop-Schnürch A. Self-nanoemulsifying drug delivery systems as novel approach for pDNA drug delivery. Int J Pharm. 2015;487:25–31.
•• **It describes the idea of using SNEDDS for pDNA delivery.**
6. Patil SD, Rhodes DG, Burgess DJ. DNA-based therapeutics and DNA delivery systems: a comprehensive review. The AAPS J. 2005;7:E61–E77.
7. Hintzen F, Perera G, Hauptstein S, et al. In vivo evaluation of an oral self-microemulsifying drug delivery system (SMEDDS) for leuprorelin. Int J Pharm. 2014;472:20–26.
8. Villar AMS, Naveros BC, Campmany ACC, et al. Design and optimization of self-nanoemulsifying drug delivery systems (SNEDDS) for enhanced dissolution of gemfibrozil. Int J Pharm. 2012;431:161–175.
9. Copolovici DM, Langel K, Eriste E, et al. Cell-penetrating peptides: design, synthesis, and applications. ACS Nano. 2014;8:1972–1994.
10. Rahmat D, Khan MI, Shahnaz G, et al. Synergistic effects of conjugating cell penetrating peptides and thiomers on non-viral transfection efficiency. Biomaterials. 2012;33:2321–2326.
11. Hyndman L, Lemoine JL, Huang L, et al. HIV-1 Tat protein transduction domain peptide facilitates gene transfer in combination with cationic liposomes. J Control Release. 2004;99:435–444.
12. Hashida H, Miyamoto M, Cho Y, et al. Fusion of HIV-1 Tat protein transduction domain to poly-lysine as a new DNA delivery tool. Brit J Cancer. 2004;90:1252–1258.
13. Zhang L, Wang X-J, Wang J, et al. An improved method of amide synthesis using acyl chlorides. Tetrahedron Lett. 2009;50:2964–2966.
14. Mahmood A, Bonengel S, Laffleur F, et al. Can thiolation render a low molecular weight polymer of just 20-kDa mucoadhesive? Drug Dev Ind Pharm. 2016;42:686–693.
15. Hintzen F, Laffleur F, Sarti F, et al. In vitro and ex vivo evaluation of an intestinal permeation enhancing self-microemulsifying drug delivery system (SMEDDS). J Drug Deliv Sci Tec. 2013;23:261–267.
• **Development and characterization of a stable self-emulsifying delivery system.**
16. Zhang J, Field CJ, Vine D, et al. Intestinal uptake and transport of vitamin B12-loaded soy protein nanoparticles. Pharm Res. 2015;32:1288–1303.
•• **Cellular internalization and uptake study methodologies are discussed.**
17. Ashraf MI, Fries D, Streif W, et al. Biopsychronology: live confocal imaging of biopsies to assess organ function. Transpl Int. 2014;27:868–876.
• **Description of the qualitative analysis of cellular internalization.**
18. Bonengel S, Prüfert F, Jelkmann M, et al. Zeta potential changing phosphorylated nanocomplexes for pDNA delivery. Int J Pharm. 2016;504:117–124.
19. Maquelin K, Kirschner C, Choo-Smith L-P, et al. Identification of medically relevant microorganisms by vibrational spectroscopy. J Microbiol Meth. 2002;51:255–271.
20. Chaffanjon P, Grisgby R, Rister E, et al. Use of real-time FTIR to characterize kinetics of amine catalysts and to develop new grades for various polyurethane applications, including low emission catalysts. J Cell Plast. 2003;39:187–210.
21. Montalbetti CA, Falque V. Amide bond formation and peptide coupling. Tetrahedron. 2005;61:10827–10852.
22. Zhao H, Lu H, Gong T, et al. Nanoemulsion loaded with lycobetaine–oleic acid ionic complex: physicochemical characteristics, in vitro, in vivo evaluation, and antitumor activity. Int J Nanomed. 2013;8:1959.
23. Cai K, Yang J, Guan M, et al. Single UV excitation of Hoechst 33342 and propidium iodide for viability assessment of rhesus monkey spermatozoa using flow cytometry. Syst Biol Reprod Mec. 2005;51:371–383.
24. Pereira De Sousa I, Moser T, Steiner C, et al. Insulin loaded mucus permeating nanoparticles: addressing the surface characteristics as feature to improve mucus permeation. Int J Pharm. 2016;500:236–244.
25. Laffleur F, Hintzen F, Shahnaz G, et al. Development and in vitro evaluation of slippery nanoparticles for enhanced diffusion through native mucus. Nanomedicine. 2014;9:387–396.
26. Khalil IA, Kogure K, Akita H, et al. Uptake pathways and subsequent intracellular trafficking in nonviral gene delivery. Pharmacol Rev. 2006;58:32–45.
27. Düzgüneş D, Nir N. Mechanisms and kinetics of liposome–cell interactions. Adv Drug Deliv Rev. 1999;40:3–18.
28. Nam HY, Kwon SM, Chung H, et al. Cellular uptake mechanism and intracellular fate of hydrophobically modified glycol chitosan nanoparticles. J Control Release. 2009;135:259–267.
29. Yumoto R, Nishikawa H, Okamoto M, et al. Clathrin-mediated endocytosis of FITC-albumin in alveolar type II epithelial cell line RLE-6TN. Am J Physiol-Lung C. 2006;290:L946–L955.
30. Dutta D, Donaldson JG. Search for inhibitors of endocytosis: intended specificity and unintended consequences. Cell Logist. 2012;2:203–208.
31. Jiang M, Gan L, Zhu C, et al. Cationic core–shell liponanoparticles for ocular gene delivery. Biomaterials. 2012;33:7621–7630.
32. Christianson HC, Belting M. Heparan sulfate proteoglycan as a cell-surface endocytosis receptor. Matrix Biol. 2014;35:51–55.
33. Ziegler A, Seelig J. Interaction of the protein transduction domain of HIV-1 TAT with heparan sulfate: binding mechanism and thermodynamic parameters. Biophys J. 2004;86(1):254–263.
•• **Mechanism of HIV-1 TAT for binding at cellular surface.**
34. Tamura M, Natori K, Kobayashi M, et al. Genogroup II noroviruses efficiently bind to heparan sulfate proteoglycan associated with the cellular membrane. J Virol. 2004;78(8):3817–3826.